Journal of ELECTRONIC MATERIALS, Vol. 44, No. 1, 2015
DOI: 10.1007/s11664-014-3481-y

Double Gaussian Distribution of Barrier Heights, Interface States, and Current Transport Mechanisms in Au/$Bi_{0.5}Na_{0.5}TiO_3$-$BaTiO_3$/*n*-GaN MIS Structure

V. RAJAGOPAL REDDY,[1,2,3] V. MANJUNATH,[1] V. JANARDHANAM,[2] CHANG-HYUN LEEM,[2] and CHEL-JONG CHOI[2,4]

1.—Department of Physics, Sri Venkateswara University, Tirupati 517 502, India. 2.—School of Semiconductor and Chemical Engineering, Semiconductor Physics Research Center (SPRC), Chonbuk National University, Jeonju 561-756, Republic of Korea. 3.—e-mail: reddy_vrg@rediffmail.com. 4.—e-mail: cjchoi@chonbuk.ac.kr

The electrical properties of Au/$Bi_{0.5}Na_{0.5}TiO_3$(BNT)-$BaTiO_3$(BT)/*n*-GaN metal–insulator–semiconductor (MIS) structures have been investigated in the temperature range from 120 K to 420 K by current–voltage and capacitance–voltage methods. The Au/BNT-BT/*n*-GaN MIS structures demonstrate nonideal behaviors indicating the presence of a nonuniform distribution of interface states. Experimental results revealed that the barrier height (Φ_{bo}), ideality factor (n), and interface state density (N_{ss}) of the Au/BNT-BT/*n*-GaN MIS structures are strongly temperature dependent. It is found that N_{ss} decreases with an increase in temperature. Further, it is observed that Φ_{bo} increases and n decreases with increasing temperature, which is attributed to barrier inhomogeneities by assuming a Gaussian distribution (GD) of barrier heights (BHs) at the interface. The temperature-dependent I–V characteristics of the Au/BNT-BT/*n*-GaN MIS structures demonstrate the presence of a double GD having mean BHs of 1.07 eV and 1.91 V and standard deviations of 0.118 V and 0.214 V. Moreover, the inhomogeneous BH is found to be correlated with N_{ss}, because Φ_{bo} becomes smaller with increasing N_{ss}. This indicates that the lateral inhomogeneity of the BH is connected to the nonuniform distribution of the density of states at the interface. Further, the conduction mechanism dominating the reverse-bias leakage current in the MIS structure is investigated.

Key words: $Bi_{0.5}Na_{0.5}TiO_3$-$BaTiO_3$ insulating layer, temperature-dependent electrical properties, density of interface states, double Gaussian distribution, barrier inhomogeneity

INTRODUCTION

Nitride-based compound semiconductors are attractive materials for fabricating high-temperature, high-frequency, and high-power electronic devices, particularly gallium nitride (GaN) due to its significant properties such as wide bandgap (3.44 V at room temperature), high breakdown field (3×10^6 V/cm), and high electron saturation velocity (2×10^7 cm/s). GaN and related compounds have been widely investigated for application in light-emitting diodes (LEDs), laser diodes (LDs), photodiodes, heterojunction field-effect transistors (HJFETs), and high-electron-mobility transistors (HEMTs).[1–8] On the other hand, GaN-based Schottky contacts suffer from abnormal leakage current that adversely affects the operation, power consumption, noise, and reliability of devices. Reduction of the leakage current can be realized by employing an insulated layer metal–semiconductor (MIS) technique. For improvement of MIS devices,

(Received April 19, 2014; accepted October 15, 2014; published online November 4, 2014)

detailed electrical characterizations of metal–insulator–GaN (MIS) interfaces must be carried out.

Various research groups have explored different metal–insulator schemes for fabrication of Schottky contacts on GaN;[9–17] For example, Tekeli et al.[11] investigated the temperature-dependent current–voltage (I–V) characteristics of inhomogeneous (Ni/Au)-$Al_{0.3}Ga_{0.7}N$/AlN/GaN heterostructures in the temperature range from 295 K to 415 K, reporting that the series resistance (R_s) plays a crucial role in affecting the forward-bias I–V curves of Schottky barrier diodes (SBDs). The values of R_s show an unusual behavior, increasing with an increase of temperature. Tsai et al.[12] fabricated Pt/GaN metal–semiconductor (MS) and Pt/SiO_2/GaN metal–insulator–semiconductor (MIS) Schottky diodes and investigated the hydrogen sensing and response characteristics of MIS diodes under different hydrogen gas concentrations over a wide temperature range in air atmosphere. They found that the adsorption time constant (τ_a) for hydrogen detection by the MS and MIS devices decreased from 25 s to 3 s and from 12 s to 2 s, respectively, as the temperature was increased from 300 K to 700 K. Arslan et al.[13] investigated the capacitance–voltage–temperature (C–V–T) and conductance–voltage (G/ω–V) characteristics of (Ni/Au)-$Al_{0.22}Ga_{0.78}N$/AlN/GaN heterostructures in the temperature range from 80 K to 390 K, reporting that the intersection behavior of C–V curves and the increase in R_s with temperature could be attributed to the lack of free charge carriers, especially at low temperatures. Demirezen et al.[14] studied the bias-dependent R_s and interface state density (N_{ss}) of the (Ni/Au)-$Al_{0.22}Ga_{0.78}N$/AlN/GaN heterostructure by admittance measurements over a wide temperature range from 80 K to 400 K. They reported that the values of both capacitance (C) and conductance (G/ω) were strongly dependent on temperature and applied bias voltage. Prasanna Lakshmi et al.[15] investigated the temperature-dependent electrical properties of the Au/SiO_2/n-GaN MIS structure in the temperature range from 120 K to 390 K. They explained the temperature dependence of the forward I–V characteristics of the Au/SiO_2/n-GaN Schottky diodes using a double Gaussian distribution of barrier heights. Zhao et al.[16] studied the current–voltage characteristics of AlGaN/GaN HEMTs in the temperature range from 223 K to 398 K, reporting that the barrier height (Φ_b), ideality factor (n), transconductance (G_m), series resistance (R_s), and leakage current values were strongly temperature dependent. Recently, Prasanna Lakshmi et al.[17] investigated the electrical characteristics of the Au/Ta_2O_5/n-GaN MIS structure for different annealing temperatures, finding that the barrier height increased upon annealing at 500°C and then slightly decreased after annealing at 600°C. They also found that the interface state density was lower for annealed compared with as-deposited contacts.

Metal–insulator–semiconductor (MIS) structures play a significant role in modern device technology. The performance and reliability of MIS devices depend on different parameters such as the surface preparation process, the formation of the insulator layer, inhomogeneities in the metal–semiconductor Schottky barrier, the density of interface states at the insulator–semiconductor interface, and the series resistance of the device.[18–22] Owing to the technical importance of MIS structures, these devices have been extensively investigated; however, very little experimental information is available yet on the barrier formation at the insulator–semiconductor interface, the temperature-dependent electrical properties, and the conduction mechanism over a wide temperature range. To the best of our knowledge, no one has investigated the electrical properties of Au/$Bi_{0.5}Na_{0.5}TiO_3$-$BaTiO_3$/n-GaN MIS structures over a wide temperature range. Therefore, in the present work, an attempt was made to fabricate and characterize the temperature-dependent electrical properties of Au/$Bi_{0.5}Na_{0.5}TiO_3$-$BaTiO_3$/n-GaN metal–insulator–semiconductor (MIS) devices formed by insertion of a thin lead-free bismuth sodium titanate ($Bi_{0.5}Na_{0.5}TiO_3$)-barium titanate ($BaTiO_3$) insulating layer between n-GaN semiconductor and Au metal. Analysis of the electrical characteristics of MS or MIS structures at room temperature only does not give detailed information about the conduction process or the nature of the barrier formation at the metal–semiconductor interface. However, temperature-dependent electrical characteristics allow one to understand the temperature dependence behavior of the main electrical parameters and the conduction mechanisms of MS or MIS structures. Hence, in this work, we investigated the detailed electrical properties of the Au/$Bi_{0.5}Na_{0.5}TiO_3$-$BaTiO_3$/n-GaN MIS structure over a wide temperature range from 120 K to 420 K for the first time. The temperature-dependent barrier characteristics of the Au/$Bi_{0.5}Na_{0.5}TiO_3$-$BaTiO_3$/n-GaN MIS structures are discussed in terms of a model of the inhomogeneities in the structure using a double Gaussian distribution of barrier heights. The reverse current conduction mechanism of the Au/$Bi_{0.5}Na_{0.5}TiO_3$-$BaTiO_3$/n-GaN MIS structure is also discussed based on the Poole–Frenkel and Schottky emission models.

EXPERIMENTAL PROCEDURES

In this work, a 2-μm-thick Si-doped GaN layer ($\sim 4.07 \times 10^{17}$ cm^{-3}) was used, grown on a c-plane Al_2O_3 sapphire substrate by metalorganic chemical vapor deposition (MOCVD). Before making ohmic contacts, the n-GaN wafer was ultrasonically degreased with warm trichloroethylene, acetone, and methanol for 5 min each and then dipped into buffered oxide etch (BOE) solution for 10 min to remove the surface oxide and rinsed in deionized (DI) water. Standard photolithography and lift-off

techniques were used to define contact electrodes. Ti (30 nm)/Al (60 nm) films were deposited on the cleaned GaN surface as ohmic contacts, followed by annealing at 750°C in N_2 for 1 min. $Bi_{0.5}Na_{0.5}TiO_3$ (BNT) and $BaTiO_3$ (BT) solutions were prepared by using the method reported in Ref. 23. Finally, the BNT and BT solutions were mixed together and stirred for an additional 12 h to obtain a yellow BNT-BT solution. Prior to BNT-BT solution spinning, the patterned layer was dipped into BOE solution for 30 s and blown dry with N_2 gas. Using the spin-coating technique (at 5000 rpm for 1 min), BNT-BT thin films were formed on the cleaned *n*-GaN substrates. Then, the wet layers were dried on a hot plate at 350°C for 10 min followed by a furnace anneal at 600°C for 1 h under O_2 atmosphere. The thickness of the BNT-BT film was found to be about 62 nm by transmission electron microscopy (TEM) measurement. This thickness was reproducible across several experimental iterations. Subsequently, 30-nm-thick Au electrodes were fabricated on the BNT-BT thin films by thermal evaporation (diode area 3.14×10^{-4} cm^2). The electrical characteristics were measured using a Keithley source measurement unit (model no. 2400) and automated deep-level transient spectrometer (DLS-83D). Current–voltage (*I*–*V*) and capacitance–voltage (*C*–*V*) characteristics were measured in the temperature range from 120 K to 420 K in steps of 30 K in the dark, with temperature controlled to accuracy of ±1 K using a temperature controller DLS-83D-1 cryostat.

RESULTS AND DISCUSSION

Electrical Properties at Different Temperatures

Figure 1 shows the forward- and reverse-bias current–voltage (*I*–*V*) characteristics of the Au/BNT-BT/*n*-GaN metal–insulator–semiconductor (MIS) structure in the temperature range from 120 K to 420 K. The measured leakage currents of the Au/BNT-BT/*n*-GaN MIS structure were in the range from 8.00×10^{-12} A (at 120 K) to 3.28×10^{-8} A (at 420 K) at −1 V. It is noted that the leakage current increases with an increase in temperature. For a Schottky diode with an interfacial insulating layer, the relation between the current (*I*) and applied voltage (*V*) is given by[24,25]

$$I = I_0 \exp\left(-a\sqrt{\chi}\delta\right) \exp\left(\frac{qV}{nkT}\right)\left[1 - \exp\left(-\frac{qV}{kT}\right)\right], \quad (1)$$

where

$$I_0 = AA^*T^2 \exp\left(\frac{-q\Phi_b}{kT}\right). \quad (2)$$

Here, I_0 is the reverse saturation current [derived from the straight-line intercept of ln(*I*) at *V* = 0], *q* is the electron charge, *n* is the ideality factor, *k* is Boltzmann's constant, *T* is the temperature in Kelvin, *A* is the contact area, *A** is the effective Richardson constant (26.4 A cm^{-2} K^{-2} for *n*-GaN),[26] and Φ_b is the Schottky barrier height (SBH). Equation 1 is similar to the standard thermionic emission (TE) equation for Schottky diodes except for the additional exponential factor $\exp(-a\chi^{1/2}\delta)$ for the characteristic of the interfacial layer. The factor $a\chi^{1/2}\delta$ is known as the tunneling factor, obtained as 1.3 from the straight-line extrapolated intercept of a plot of $\ln(I_0/T^2)$ versus $1000/nT$ (not shown here),[27] where δ is the thickness of the interfacial insulator layer, $a = (4\pi/h)(2m^*)^{1/2} = 0.481$ $eV^{-1/2}$ $Å^{-1}$ is a constant obtained using the effective tunneling mass of an electron $m^* = 0.22m_0$ (for GaN), m_0 is the electron rest mass, and $h = 4.135 \times 10^{-15}$ eV s. χ is the mean tunneling barrier presented by the interfacial layer and is calculated to be 0.196 eV. The Schottky barrier height Φ_{ap} at temperature *T*, with an interfacial insulator layer of thickness δ, is given by[24]

$$\Phi_{ap} = \Phi_b + \frac{akT\delta\sqrt{\chi}}{q}. \quad (3)$$

The ideality factor was estimated from the slope of the linear region of forward-bias ln(*I*)–*V* plots. The barrier height Φ_{ap} and *n* values obtained for the Au/BNT-BT/*n*-GaN MIS structure were 0.46 eV and 3.23 at 120 K and 1.40 eV and 1.31 at 420 K, respectively. Experimental results reveal that the ideality factor decreases with increasing temperature, which is attributed to the current transport across the metal–semiconductor interface, which is a temperature-activated process; electrons at low temperatures are able to surmount the lower barriers.[28–30] Thus, the current transport at low temperatures will be dominated by the current flowing through the patches of lower Schottky barrier

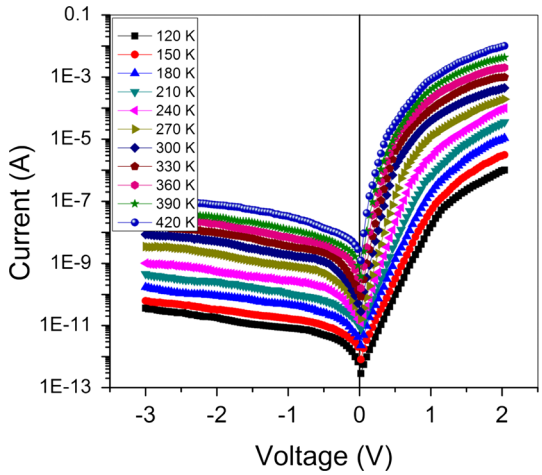

Fig. 1. Forward- and reverse-bias current–voltage (*I*–*V*) characteristics of the Au/BNT-BT/*n*-GaN MIS structure in the temperature range from 120 K to 420 K in steps of 30 K.

height.[29,31] It can be seen that the SBH values of the Au/BNT-BT/*n*-GaN MIS structure determined from the *I*–*V* characteristics show an unusual behavior with increase of temperature. Such temperature dependence of the SBH is attributed to barrier inhomogeneity at the metal–semiconductor junction.

The experimental reverse-bias C^{-2}–V characteristics of the Au/BNT-BT/*n*-GaN MIS structure in the temperature range from 120 K to 420 K in steps of 30 K are shown in Fig. 2. The junction capacitance was measured at frequency of 1 MHz. In Schottky diodes, the depletion capacitance is expressed as[18]

$$\frac{1}{C^2} = \frac{2(V_{bi} + V_r - kT/q)}{q\epsilon_s\epsilon_0 A^2 N_d}, \qquad (4)$$

where V_{bi} is the built-in voltage determined from the extrapolation of the $1/C^2$ plot to the voltage axis, V_r is the reverse voltage, ε_s is the static dielectric constant (equal to 9.5 for *n*-GaN), $\varepsilon_0 = 8.85 \times 10^{-14}$ F/cm, and N_d is the donor concentration. N_d is related to the slope of the $1/C^2$ versus V curve and can be determined from the expression $N_d = 2/q\varepsilon_s\varepsilon_0 A^2[1/(d(C^{-2})/dV)]$. The barrier height is given by the equation $\Phi_{C-V} = V_0 + V_n + kT/q$, where $V_n = (kT/q)\ln(N_c/N_d)$. The density of states at the conduction-band edge is given by $N_c = 2(2\pi m^* kT/h^2)^{3/2}$, being 2.6×10^{18} cm^{-3} for *n*-GaN at room temperature, where $m^* = 0.22m_0$. From reverse-bias C^{-2}–V characteristics, the donor concentration (N_d) was determined as a function of temperature, varying from 3.47×10^{17} cm^{-3} at 120 K to 5.03×10^{17} cm^{-3} at 420 K. It is noted that the N_d of the *n*-GaN slightly decreases as the temperature decreases. At low temperatures, almost all impurities are frozen out, resulting in a strong increase in the series resistance (R_s) of the diode, which makes the measured capacitance appear smaller. More electrons may be frozen at the donor level in the freeze-out region, and conduction mechanisms in the freeze-out regions are complex. Since the donor concentration decreases, the capacitance also decreases with decreasing temperature. The calculated barrier heights of the Au/BNT-BT/*n*-GaN MIS structure are 1.31 eV at 120 K and 1.02 eV at 420 K, respectively. It is noted that the SBH values derived from *I*–*V* measurements differ from those estimated from *C*–*V* measurements. This may be due to the different nature of the *I*–*V* and *C*–*V* measurements. The capacitance C is insensitive to potential fluctuations on length scales smaller than the space-charge region, and the *C*–*V* measurements average over the whole Schottky area, resulting in a homogeneous SBH. Accordingly, the SBH determined from the zero-bias intercept assuming TE as a current transport mechanism is well below the *C*–*V* or flat-band measured BH and the weighted arithmetic average SBH.[32,33] The direct current (DC) I across the interface depends exponentially on barrier height and thus sensitively on the detailed distribution of the surface state density at the interface. Normally, *C*–*V* measurements are less susceptible to dislocations or pinholes, hence the estimated BH is considered more reliable. The depletion width can be altered by the interface defects if they are deeper into the space-charge region.

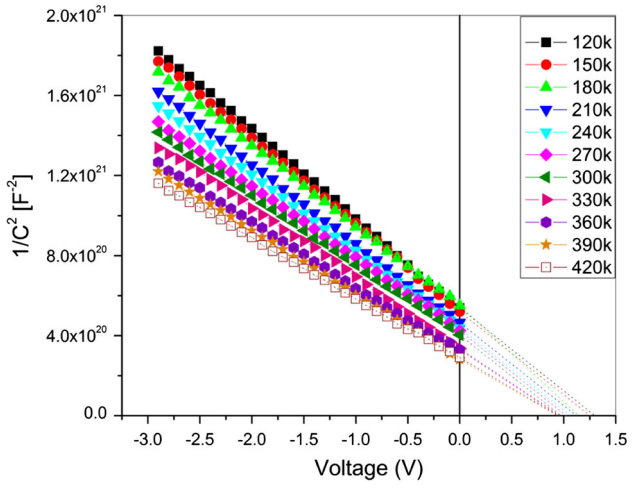

Fig. 2. Reverse-bias C^{-2}–V characteristics of the Au/BNT-BT/*n*-GaN MIS structure in the temperature range from 120 K to 420 K.

Density of Interface States

The bias dependence of the Schottky barrier height (SBH) is described in terms of the dependence of the ideality factor on the applied bias due to surface states, and the BH shift with forward bias V is given by[19,34,35]

$$\Phi_e(V) - \Phi_{bo} = \left(1 - \frac{1}{n(V)}\right)(V - IR_s). \qquad (5)$$

The ideality factor can be directly estimated from Eq. 1 for each measuring temperature at any given forward bias from the slope of the ln(*I*)–*V* characteristics as $n(V) = (q/kT)[dV/d\ln(I)]$. Our Au/BNT-BT/*n*-GaN MIS structures clearly indicate that the ideality factor is larger than unity in the linear region. The nonlinear region of the forward-bias semilog *I*–*V* plots shows a deviation in the ideality factor at high current, which is due to the interfacial layer thickness, the interface state density, and series resistance. It can be concluded that the BH and other characteristic parameters are mainly controlled by the interface states and play a significant role at interlayer–semiconductor interfaces. The density distribution of interface states (N_{ss}) in equilibrium with the semiconductor can be estimated from the forward-bias *I*–*V* data by taking the voltage-dependent ideality factor $n(V,T)$ with effective barrier height $\Phi_b(V,T)$. The parameters $n(V,T)$ and $\Phi_b(V,T)$ can be calculated from the following equations:[20]

$$n(V) = 1 + \frac{\delta}{\epsilon_i}\left[\frac{\epsilon_s}{W_d} + q \cdot N_{ss}\right], \quad (6)$$

$$\Phi_b(V,T) = \Phi_{bo}^{IV} + \beta V = \Phi_{bo}^{IV} + \left(1 - \frac{1}{n(V,T)}\right). \quad (7)$$

For a metal–semiconductor (MS) diode having interface states N_{ss} in equilibrium with the semiconductor, the ideality factor n becomes greater than unity as proposed by Card and Rhoderick,[20] and the interface state density N_{ss} can be expressed as

$$N_{ss}(V) = \frac{1}{q}\left[\frac{\epsilon_i}{\delta}(n(V,T) - 1) - \frac{\epsilon_s}{W_d}\right], \quad (8)$$

where W_d is the width of the space-charge region, ε_i and ε_s are the permittivity of the interfacial insulator layer and the semiconductor, respectively, and β [=$d\Phi_{eff}/dV$ = 1 − 1/$n(V)$] is the change in the effective BH with bias voltage. Also, in n-type semiconductors, the energy of interface states E_{ss} with respect to the conduction-band edge, E_c, at the semiconductor surface is given by

$$E_c - E_{ss} = q(\Phi_e - V), \quad (9)$$

where Φ_e is the effective barrier height of the n-type semiconductor. Substituting the values of the voltage dependence of $n(V)$, δ, and W_d (as calculated from $1/C^2$–V characteristics) into Eq. 6, the values of N_{ss} as a function of $(E_c - E_{ss})$ are obtained (Fig. 3). It is clearly seen from Fig. 3 that N_{ss} exhibits exponential growth from the midgap of GaN toward the bottom of the conduction-band edge for all temperatures. The magnitude of the interface state density (N_{ss}) varies from 5.15×10^{12} eV^{-1} cm^{-2} (E_c − 0.30 eV) to 3.45×10^{12} eV^{-1} cm^{-2} (E_c − 0.45 eV) at 120 K, and from 2.94×10^{12} eV^{-1} cm^{-2} (E_c − 0.82 eV) to 5.43×10^{11} eV^{-1} cm^{-2} (E_c − 1.40 eV) at 420 K. These values are more consistent with other results reported in literature.[15,17] The N_{ss} value of the Au/BNT-BT/n-GaN MIS structure decreases with increasing $E_c - E_{ss}$ as a function of temperature. Such behavior of N_{ss} has been explained based on variation of the ideality factor as a function of temperature due to lateral inhomogeneities of the barrier height at the metal–semiconductor interface.[36] According to Akkal,[37] the increase of N_{ss} with decreasing temperature is a result of molecular restructuring and reordering of the metal–semiconductor interface under the influence of temperature.

Barrier Inhomogeneities

The ideality factor of the Au/BNT-BT/n-GaN MIS structure may increase with a decrease in temperature over the distribution of low Schottky barrier height (SBH). A plot of the experimental zero-bias BH versus the ideality factor is shown in Fig. 4. By using Tung's theoretical approach, Schmitsdorf et al.[38] found a linear correlation between the experimental zero-bias BH and the ideality factor. As can be seen from Fig. 4, there are two linear regions between the experimental BHs and ideality factor of our MIS structure, which can be explained by the lateral inhomogeneity of the BHs.[30,39] The extrapolation of the experimental BH at the ideality factor n = 1 gives a BH value of 1.59 eV in the distribution 1 (210 K to 420 K) and 1.13 eV in the distribution 2 (120 K to 210 K). Thus, it is noticed that there is a significant decrease in the value of the zero-bias BH and an increase in the value of the ideality factor especially at low temperature, which may be due to barrier inhomogeneities. These results confirm that the current transport is not due to TE in our MIS structure. Moreover, the results indicate the presence of a double Gaussian distribution (GD) of BHs, namely Gaussian distribution 1 (GD1) and Gaussian distribution 2 (GD2), in the contact area.

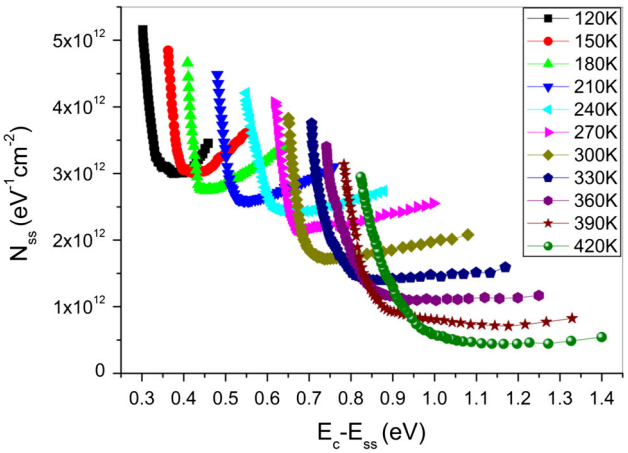

Fig. 3. N_{ss} versus E_c – E_{ss} for the Au/BNT-BT/n-GaN MIS structure at temperatures ranging from 120 K to 420 K.

To explain the SBH inhomogeneity at the metal–semiconductor interface, we assume the model of lateral SBH distribution with Gaussian distribution (GD) over the BHs proposed by Werner and Guttler.[39] The GD of the BHs with mean value $\overline{\Phi}_{bo}$ and standard deviation σ_o yields the following expression for the BH:

$$\Phi_{ap} = \overline{\Phi_{bo}}(T = 0) - \frac{q\sigma_o^2}{2kT} \quad (10)$$

and

$$\left(\frac{1}{n_{ap}} - 1\right) = -\rho_2 + \frac{q\rho_3}{2kT}, \quad (11)$$

where Φ_{ap} is the apparent barrier height, n_{ap} is the apparent ideality factor, and ρ_2 and ρ_3 quantify the voltage deformation of the barrier height distribution,

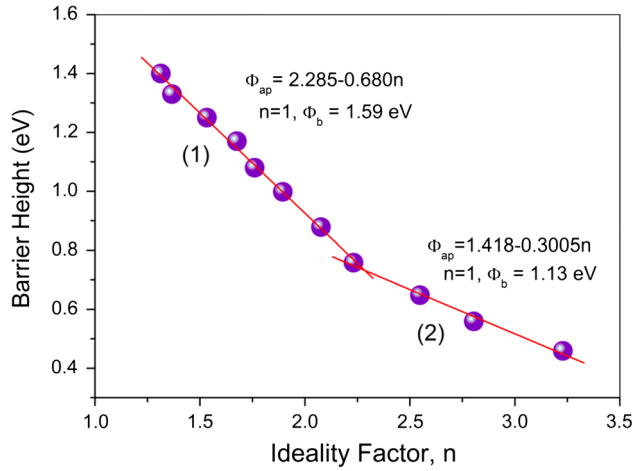

Fig. 4. Schottky barrier heights versus ideality factor of the Au/BNT-BT/*n*-GaN MIS structure in the temperature range from 120 K to 420 K.

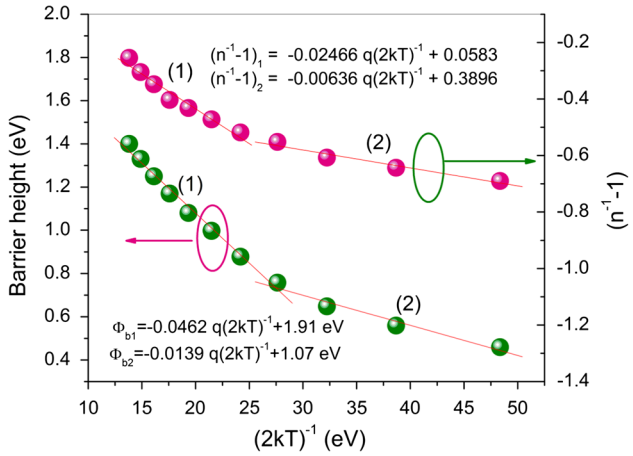

Fig. 5. Zero-bias apparent barrier height and ideality factor versus 1/2*kT* curves for the Au/BNT-BT/*n*-GaN MIS structure according to two Gaussian distributions of BHs. The data show linear variation in the two temperature ranges with a transition around 210 K.

which may depend on temperature.[39] The temperature dependence of σ_o is usually small and can be neglected.[40] According to Eq. 10, a plot of Φ_{ap} versus $1/2kT$ should be a straight line with the intercept at the ordinate estimating the zero-bias mean value of SBH ($\overline{\Phi}_{bo}$) and the slope giving the zero-bias standard deviation (σ_o). For the Au/BNT-BT/*n*-GaN MIS structure, the experimental plots of Φ_{ap} versus $q/2kT$ (Fig. 5) exhibit two linear regions. This observation indicates the presence of two Gaussian distributions of SBHs in the contact area. The intercepts and slopes of these straight lines give two sets of values of $\overline{\Phi}_{bo}$ and σ_o as 1.91 eV and 0.215 eV in the temperature range from 210 K to 420 K (distribution 1), and 1.07 eV and 0.118 eV in the temperature range from 120 K to 210 K (distribution 2). Moreover, Chand and Kumar[40] indicated the existence of a double Gaussian distribution in metal–semiconductor contacts which could be attributed to the nature of the inhomogeneities themselves, which may involve variation in the interface phase composition, interface quality, electrical charges, nonstoichiometry, etc. These are important enough to electrically control the *I–V* characteristics of the Schottky diodes, particularly at low temperatures. Thus, *I–V* measurements at very low temperatures can shed light on the nature of barrier inhomogeneities that exist in the contact area. Also, these results have shown that the temperature dependence characteristics of the Au/BNT-BT/*n*-GaN MIS structure can be explained on the basis of a TE mechanism with a double GD of BHs.

In addition, the plot of $(1/n_{ap} - 1)$ versus $q/2kT$ (Fig. 5) should be a straight line that gives the voltage coefficients ρ_2 and ρ_3 from the intercept and slope, respectively. The ρ_2 values obtained are $\rho_2 = -0.232$ V in the range of 210 K to 420 K (distribution 1) and $\rho_2 = -0.322$ V in the range of 120 K to 210 K (distribution 2), whereas the values of ρ_3 obtained from the slopes are −0.0286 V in the range of 210 K to 420 K (distribution 1) and −0.0079 V in the range of 120 K to 210 K (distribution 2). The linear behavior of the $(1/n_{ap} - 1)$ versus $q/2kT$ plot demonstrates that the ideality factor does indeed express the voltage deformation of the GD of the SBH. According to these results, this inhomogeneity and potential fluctuation in the barrier dramatically affect the low-temperature *I–V* characteristics. It can also be noted from the $(1/n_{ap} - 1)$ versus $q/2kT$ plot that the ρ_3 value in distribution 1 is larger than that in distribution 2. Therefore, it can be said that distribution 2 at very low temperatures may possibly occur due to some phase change on cooling below a certain temperature. A similar behavior with a double GD has been observed in the Au/SiO_2/*n*-GaN MIS structure[15] and Al/TiO_2/*p*-Si MIS structure.[41]

Taking into account the barrier inhomogeneity, a modified Richardson plot can be obtained by combining Eqs. 2 and 10 to yield the following expression:

$$\ln\left(\frac{I_o}{T^2}\right) - \left(\frac{q^2\sigma_o^2}{2k^2T^2}\right) = \ln(AA^*) - \frac{q\overline{\Phi}_{bo}}{kT}. \qquad (12)$$

Figure 6 shows such a modified $\ln(I_o/T^2) - q^2\sigma_o^2/2k^2T^2$ versus $1000/T$ plot. The mean BH ($\overline{\Phi}_{bo}$) and effective Richardson constant (A^*) are given by linear fitting to these curves. It can be seen from Fig. 6 that there are two linear regions with a transition occurring at 210 K; the slope of these linear regions directly yields the mean BHs ($\overline{\Phi}_{bo}$), and the intercept (=ln AA^*) at the ordinate estimates A^* for a given rectifier contact area. Thus, the $\ln(I_o/T^2) - q^2\sigma_o^2/2k^2T^2$ values are estimated for both values of σ_o obtained in the temperature ranges of 120 K to 210 K and 210 K to 420 K. The values of the zero-bias mean BH ($\overline{\Phi}_{bo}$) and effective A^* are found to be 0.98 eV and 1.86 A cm^{-2} K^{-2} in the temperature range of 120 K to 210 K (distribution 2) and 1.79 eV and 45.05 A cm^{-2} K^{-2} in the temperature range of 210 K to 420 K (distribution 1). The zero-bias mean

BH ($\overline{\Phi}_{bo}$) values estimated from the $\ln(I_o/T^2) - q^2\sigma_o^2/2k^2T^2$ versus $1000/T$ plot are close to the mean BHs obtained from the Φ_{ap} versus $q/2kT$ plots in Fig. 5. Specifically, the A^* value of 23.71 A cm^{-2} K^{-2} as found in the temperature range of 210 K to 420 K is close to the theoretical value of 26.4 A cm^{-2} K^{-2} for n-type GaN.

If the origin of the inhomogeneities of SBH is considered to be the nonuniform distribution of interface state density, the measured SBH is more or less equal to the homogeneous SBH barrier, provided the interface state density (N_{ss}) is very low. This can be confirmed by plotting the measured SBH as a function of the corresponding calculated interface states at different temperatures. Figure 7a shows the variation of barrier height versus interface state density for the Au/BNT-BT/n-GaN MIS structure. It can be clearly observed from Fig. 7a that the SBH depends on the interface state density and that the apparent barrier height becomes lower with increasing interface state density. The SBH increases linearly with decreasing interface state density, with the intercept at the ordinate axis yielding the image-force-controlled zero-bias homogeneous SBH. From the linear extrapolation of SBH versus N_{ss} plots to $N_{ss} \approx 0$, a SBH of 1.50 eV is obtained for the Au/BNT-BT/n-GaN MIS structure. This SBH value is in reasonable agreement with the homogeneous SBH values determined in the temperature range of 210 K to 420 K from the plot of Φ_b versus n. The slight difference of 0.09 eV between the values obtained from the plot of Φ_b versus n (1.59 eV) and that extrapolated at $N_{ss} \approx 0$ from the plot of SBH versus N_{ss} (1.50 eV) can be explained by the effect of image force lowering. Indeed, linear extrapolation of the experimentally measured BH versus N_{ss} curves gives the image-force-lowered BH of laterally homogeneous contacts.[42] Likewise, extrapolation of the linear fits of the ideality factor n versus N_{ss} (Fig. 7b) to $N_{ss} \approx 0$ gives an ideality factor of 1.02, which corresponds to the image-force-controlled ideality factor (n_{if}) of the homogeneous MIS structure. Interestingly, the rate of variation of BH and n with N_{ss} is approximately the same. These results indicate that the lateral barrier inhomogeneities at the interface are connected to the nonuniform distribution of $N_{ss}(E)$ at the interface. This may be attributed to the native defects at and close to the metal–GaN interface.[35]

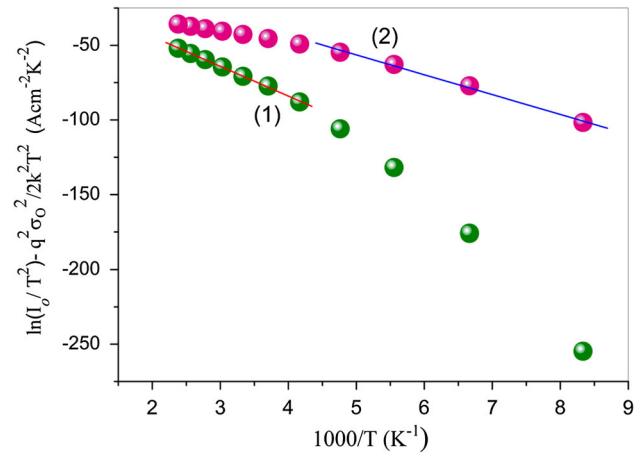

Fig. 6. Modified Richardson plot of $\ln(I_o/T^2) - (q^2\sigma_o^2/2k^2T^2)$ versus $10^3/T$ for the Au/BNT-BT/n-GaN MIS structure according to the double GD of BHs.

Current Transport Mechanisms

The reverse leakage current mechanisms in the Au/BNT-BT/n-GaN MIS structure were investigated using the electric field dependence by considering the Poole–Frenkel emission and Schottky barrier lowering mechanisms across the junction. The field-dependent effects are more evident at reverse biases due to the larger electric fields involved for such bias. Generally, carrier

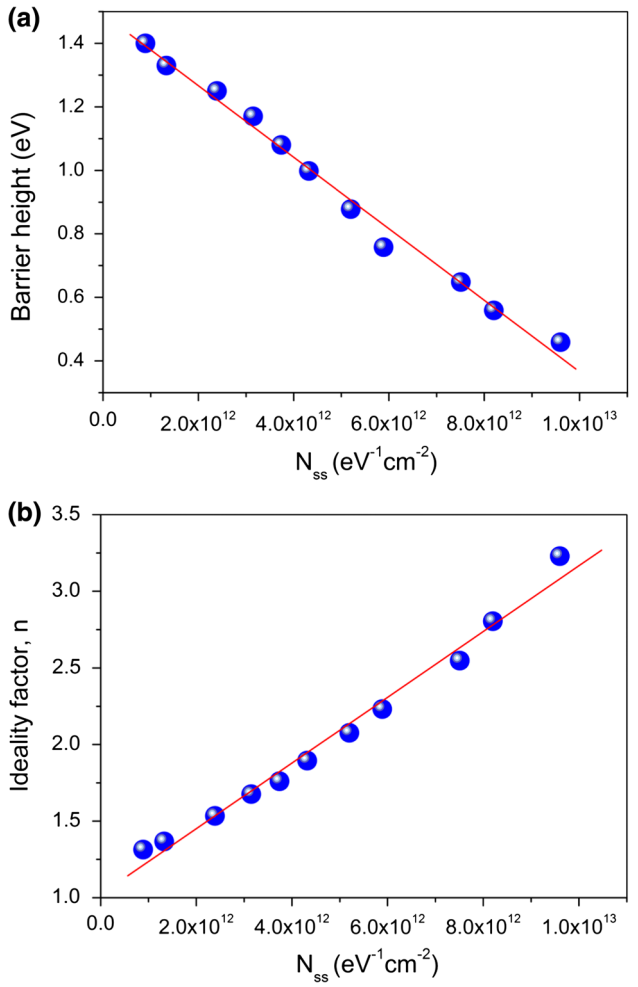

Fig. 7. (a) Zero-bias Schottky barrier height Φ_{bo} versus interface state density N_{ss} for the Au/BNT-BT/n-GaN MIS structure, and (b) ideality factors n versus interface state density N_{ss} for the Au/BNT-BT/n-GaN MIS structure.

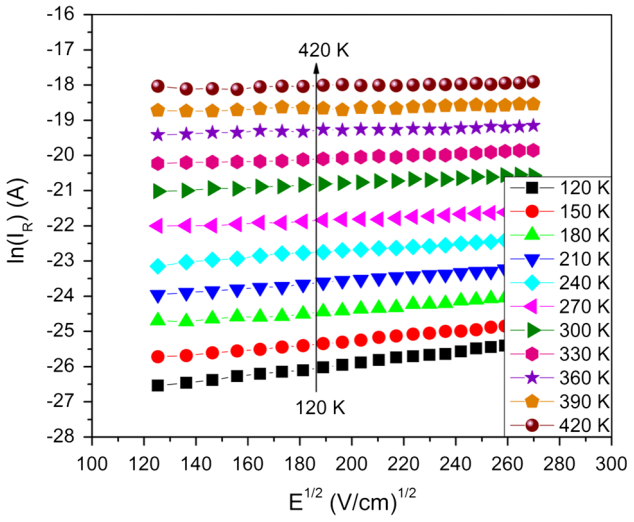

Fig. 8. $\ln(I_R)$ versus $E^{1/2}$ for the Au/BNT-BT/*n*-GaN MIS structure at temperatures ranging from 120 K to 420 K.

recombination in the depletion layer and image force lowering of the BH often dominate the reverse characteristics of devices because the reverse bias increases the electric field in the junction. The current through the diode when dominated by the Poole–Frenkel effect is given by[43–45]

$$I_R = I_o \exp\left(\frac{\beta_{PF}}{kT}\sqrt{E}\right). \quad (13)$$

For the Schottky effect,

$$I_R = AA^*T^2 \exp\left(\frac{\beta_S}{kT}\sqrt{E}\right), \quad (14)$$

where β_{PF} and β_S are the Poole–Frenkel and Schottky field-lowering coefficients, respectively. The theoretical values for β_{PF} and β_S are given by

$$2\beta_S = \beta_{PF} = \left(\frac{q^3}{\pi\epsilon}\right)^{1/2}. \quad (15)$$

From the measured values of the field-lowering coefficients, domination by the Poole–Frenkel or Schottky effect can be determined. The Poole–Frenkel field-lowering coefficient (β_{PF}) is always twice the value of the Schottky field-lowering coefficient (β_S). The theoretical values of the field-lowering coefficients β_{PF} and β_S for the Au/BNT-BT/*n*-GaN MIS structure obtained from Eq. 14 are $\beta_{PF} = 3.09 \times 10^{-5}$ eV/m$^{1/2}$ V$^{-1/2}$ and $\beta_S = 1.54 \times 10^{-5}$ eV/m$^{1/2}$ V$^{-1/2}$.

Figure 8 shows a plot of $\ln(I_R)$ versus $E^{1/2}$ for the Au/BNT-BT/*n*-GaN MIS structure at different temperatures. The experimental slopes estimated from the fit to the data for the Au/BNT-BT/*n*-GaN MIS structure are 3.76×10^{-5} eV/m$^{1/2}$ V$^{-1/2}$, 3.60×10^{-5} eV/m$^{1/2}$ V$^{-1/2}$, 3.40×10^{-5} eV/m$^{1/2}$ V$^{-1/2}$, 3.35×10^{-5} eV/m$^{1/2}$ V$^{-1/2}$, 3.29×10^{-5} eV/m$^{1/2}$ V$^{-1/2}$, 3.10×10^{-5} eV/m$^{1/2}$ V$^{-1/2}$, 2.96×10^{-5} eV/m$^{1/2}$ V$^{-1/2}$, 2.77×10^{-5} eV/m$^{1/2}$ V$^{-1/2}$, 1.74×10^{-5} eV/m$^{1/2}$ V$^{-1/2}$, 1.59×10^{-5} eV/m$^{1/2}$ V$^{-1/2}$, and 1.26×10^{-5} eV/m$^{1/2}$ V$^{-1/2}$ for 120 K, 150 K, 180 K, 210 K, 240 K, 270 K, 300 K, 330 K, 360 K, 390 K, and 420 K, respectively. The estimated slope values for the Au/BNT-BT/*n*-GaN MIS structure closely match the theoretical slopes of the Poole–Frenkel mechanism in the temperature range of 120 K to 330 K and Schottky emission in the temperature range of 360 K to 420 K. By comparing the experimental and theoretical slopes, it is revealed that the experimental slopes estimated in the low-temperature region ($T \le 330$ K) are closer to the Poole–Frenkel field-lowering coefficient (β_{PF}), whereas the experimental slopes in the higher-temperature region ($T \ge 360$ K) are closer to the Schottky field-lowering coefficient (β_S). From these observations, the leakage current is found to be dominated by Poole–Frenkel emission in the lower-temperature region ($T < 330$ K) while Schottky emission is dominant in the higher-temperature region ($T > 360$ K). Furthermore, the conduction mechanism of the Au/BNT-BT/*n*-GaN MIS structure shows a transition from Poole–Frenkel emission to Schottky emission in the temperature range from 330 K to 360 K.

CONCLUSIONS

The electrical properties of the Au/BNT-BT/*n*-GaN metal–insulator–semiconductor (MIS) structure have been investigated in the temperature range from 120 K to 420 K in steps of 30 K. Calculations showed that the SBH (Φ_{bo}) and the ideality factor *n* of the Au/BNT-BT/*n*-GaN MIS structure are 0.46 eV (*I–V*) or 1.31 eV (*C–V*) and 3.23 at 120 K, and 1.40 eV (*I–V*) or 1.02 eV (*C–V*) and 1.31 at 420 K, respectively. The Φ_{bo} and *n* values of the Au/BNT-BT/*n*-GaN MIS structure are found to be strongly temperature dependent, with an increase in barrier height and a decrease in ideality factor with increasing temperature. Also, the interface state density N_{ss} has been estimated from the bias and temperature dependence of the barrier height $\Phi_b(V,T)$ and ideality factor $n(V,T)$, revealing that N_{ss} decreases with an increase in temperature. Experimental results for the Au/BNT-BT/*n*-GaN MIS structure demonstrate the existence of a double Gaussian distribution with mean barrier heights ($\overline{\Phi}_{bo}$) of 1.07 eV and 1.91 eV and standard deviations (σ_o) of 0.118 V and 0.215 V, respectively. Then, from a modified $\ln(I_o/T^2) - (q^2\sigma_o^2/2k^2T^2)$ versus $10^3/T$ plot, the values of $\overline{\Phi}_{bo}$ and A^* can be estimated to be 0.98 eV and 1.86 A cm^{-2} K^{-2} (120 K to 210 K), and 1.79 eV and 45.05 A cm^{-2} K^{-2} (210 K to 420 K), respectively. An A^* value of 45.05 A cm^{-2} K^{-2} is obtained in the temperature range of 210 K to 420 K, being closer to the theoretical value of 26.4 A cm^{-2} K^{-2} for *n*-type GaN. Furthermore, a linear correlation is observed between the zero-bias BH (Φ_{bo}) and the interface state density (N_{ss}). The extrapolated value of SBH

obtained from the plot of Φ_{bo} versus N_{ss} is in reasonable agreement with homogeneous SBH values obtained from the plot of Φ_{bo} versus n in the temperature range of 210 K to 420 K. Moreover, investigations reveal that Poole–Frenkel emission accounts for the reverse leakage current at 120 K to 330 K, while Schottky emission is the dominant mechanism at high temperatures (360 K to 420 K). It is noted that there is a change of the conduction mechanism from Poole–Frenkel to Schottky emission at 330 K to 360 K.

ACKNOWLEDGEMENTS

This work was supported by the Converging Research Center Program (2014M3C1A8048834) through the Ministry of Science, ICT & Future Planning, Republic of Korea. It was also was supported by a grant from the R&D Program for Industrial Core Technology funded by the Ministry of Trade, Industry and Energy (MOTIE), Republic of Korea (Grant No. 10045216).

REFERENCES

1. R. Vetury, N.Q. Zhang, S. Keller, and U.K. Mishra, *IEEE Trans. Electron Devices* 48, 560 (2001).
2. S.C. Jain, M. Willander, J. Narayan, and R.V. Overstraeten, *J. Appl. Phys.* 87, 965 (2000).
3. J. Kolnik, I.H. Oguzman, F. Brennan, R. Wang, and P. Paul Ruden, *J. Appl. Phys.* 81, 726 (1997).
4. Y.J. Lee, J.M. Hwang, T.C. Hsu, M.H. Hsieh, M.J. Jou, B.J. Lee, T.C. Lu, H.C. Kuo, and S.C. Wang, *IEEE Photonics Technol. Lett.* 18, 1152 (2006).
5. T. Miyajima, T. Tojyo, T. Asano, K. Yanashima, S. Kijima, T. Hino, M. Takeya, S. Uchida, S. Tomiya, K. Funato, T. Asatsuma, T. Kobayashi, and M. Ikeda, *J. Phys.: Condens. Matter* 13, 7099 (2001).
6. J.C. Carrano, D.J.H. Lambert, C.J. Eiting, C.J. Collins, T. Li, S. Wang, B. Yang, A.L. Beck, R.D. Dupuis, and J.C. Campbell, *Appl. Phys. Lett.* 76, 24 (1999).
7. Y. Ohno and M. Kuzuhara, *IEEE Trans. Electron Devices* 48, 517 (2001).
8. L.H. Huang, S.H. Yeh, and C.T. Lee, *Appl. Phys. Lett.* 93, 043511 (2008).
9. T. Hashizume, E. Alekseev, D. Pavlidis, K.S. Boutros, and J. Redwing, *J. Appl. Phys.* 88, 1983 (2000).
10. Y. Nakano and T. Jimbo, *Appl. Phys. Lett.* 80, 4756 (2002).
11. Z. Tekeli, S. Altindal, M. Cakmak, S. Ozcelik, D. Caliskan, and E. Ozbay, *J. Appl. Phys.* 102, 054510 (2007).
12. T.-H. Tsai, J.-R. Huang, K.-W. Lin, W.-C. Hsu, H.-I. Chen, and W.-C. Liu, *Sens. Actuators B* 129, 292 (2008).
13. E. Arslan, Y. Safak, S. Altindal, O. Kelekci, and E. Ozbay, *J. Non-Cryst. Solids* 356, 1006 (2010).
14. S. Demirezen and S. Altindal, *Phys. B* 405, 1130 (2010).
15. B. Prasanna Lakshmi, M. Siva Pratap Reddy, A. Ashok Kumar, and V. Rajagopal Reddy, *Curr. Appl. Phys.* 12, 765 (2012).
16. M. Zhao, X.Y. Liu, Y.K. Zheng, Y. Li, and S. Ouyang, *Mater. Sci. Eng. B* 178, 465 (2013).
17. B. Prasanna Lakshmi, V. Rajagopal Reddy, V. Janardhanam, M. Siva Pratap Reddy, and Jung-Hee Lee, *Appl. Phys. A* 113, 713 (2013).
18. S.M. Sze and K. Ng Kwok, *Physics of Semiconductor Devices* (New Jersey: Wiley, 2007).
19. E.H. Rhoderick and R.H. Williams, *Metal–Semiconductor Contacts* (Oxford: Clarendon, 1978).
20. H.C. Card and E.H. Rhoderick, *J. Phys. D Appl. Phys.* 4, 1589 (1970).
21. A. Singh, *Solid-State Electron.* 28, 223 (1985).
22. P. Chattopadhyay and B. Raychaudhuri, *Solid-State Electron.* 36, 605 (1993).
23. S.K. Acharya, L.S. Kwon, H.J. Hwan, Y.Y. Ho, K.B. Hee, and A.B. Guk, *J. Alloys Compd.* 540, 204 (2012).
24. S. Chand and S. Bala, *Phys. B* 390, 179 (2007).
25. M.K. Hudait and B. Krupanidhi, *Mater. Sci. Eng. B* B87, 141 (2001).
26. X.J. Wang and L. He, *J. Electron. Mater.* 27, 1272 (1998).
27. S. Altindal, S. Karadeniz, N. Tugluoglu, and a Tataroglu, *Solid State Electron.* 47, 1847 (2003).
28. S. Shankar Naik and V. Rajagopal Reddy, *Superlattices Microstruct.* 48, 330 (2010).
29. S. Chand and J. Kumar, *Appl. Phys. A Mater. Sci. Process.* 65, 497 (1997).
30. S. Zhu, R.L. Van Meirhaeghe, C. Detavernier, G.P. Ru, B.Z. Li, and F. Cardon, *Solid State Commun.* 112, 611 (1999).
31. A. Tataroglu, S. Altindal, and M.M. Bulbul, *Microelectron. Eng.* 81, 140 (2005).
32. J.H. Werner and H.H. Guttler, *J. Appl. Phys.* 69, 1522 (1991).
33. J.P. Sullivan, R.T. Tung, M.R. Pinto, and W.R. Graham, *J. Appl. Phys.* 70, 7403 (1991).
34. A. Turut, M. Saglam, H. Efeoglu, N. Yalcin, M. Yildirim, and B. Abay, *Phys. B* 205, 41 (1995).
35. M. Mamor, *J. Phys.: Condens. Matter* 21, 335802 (2009).
36. N. Ucar, A.F. Ozdemir, D.A. Aldemir, S. Cakmak, A. Calik, H. Yildiz, and F. Cimilli, *Superlattices Microstruct.* 47, 586 (2010).
37. B. Akkal, Z. Benemara, A. Boudissa, N.B. Bouiadjea, M. Amrani, and L. Bideux, *Mater. Sci. Eng. B* 55, 162 (1998).
38. R.F. Schmitsdorf, T.U. Kampen, and W. Monch, *Appl. Surf. Sci.* 324, 249 (1995).
39. J.H. Werner and H.H. Guttler, *J. Appl. Phys.* 73, 1315 (1993).
40. S. Chand and J. Kumar, *Semicond. Sci. Technol.* 11, 1203 (1996).
41. O. Pakma, N. Serin, T. Serin, and S. Altındal, *J. Appl. Phys.* 104, 014501 (2008).
42. S.C. Jain, M. Willander, J. Narayan, and R. Van Overstraeten, *J. Appl. Phys.* 87, 965 (2000).
43. W.Z. Schottky, *Physik* 15, 872 (1914).
44. J. Frenkel, *Phys. Rev.* 54, 647 (1938).
45. C.A. Mead, *Phys. Rev.* 128, 2088 (1962).